

Modeling and Simulation of Dynamic Recrystallization Behaviors of 7085 Aluminum Alloy During Hot Deformation Using Cellular Automata Method



Jie Zhang, Zhihui Li, Shuhui Huang, Xiwu Li, Lizhen Yan, Hongwei Yan, Hongwei Liu, Yongan Zhang and Baiqing Xiong

Abstract Cellular Automata (CA) method can be used to simulate the microstructure evolution. The parameters of the CA model and thermal deformation parameters are input to the CA model as important data. The hot deformation behavior was studied by means of a hot simulating test on Geleeble-1500 experiment machine. The range of thermal deformation temperature is 623–723 K, the range of strain rate is $0.001\text{--}1\text{ s}^{-1}$ and the maximum true strain is 0.91. Analysis of microstructure of average grain size and recrystallization fraction by optical

J. Zhang · Z. Li (✉) · S. Huang · X. Li · L. Yan · H. Yan · H. Liu · Y. Zhang · B. Xiong
State Key Laboratory of Nonferrous Metals and Processes, General Research Institute
for Nonferrous Metals, Beijing 100088, China
e-mail: lzh@grinm.com

J. Zhang
e-mail: jiezhang_china@163.com

S. Huang
e-mail: hithuang@126.com

X. Li
e-mail: xiwuli@163.com

L. Yan
e-mail: yanlizhentnm@163.com

H. Yan
e-mail: yanhongwei@grinm.com

H. Liu
e-mail: lhw@grinm.com

Y. Zhang
e-mail: zhangyongansk12017@163.com

B. Xiong
e-mail: xiongbq@grinm.com

microscope (OM) and electron backscatter diffraction (EBSD). CA model was used to study the effects of strain, strain rate and deformation temperature on the deformed microstructure. The simulation results are validated by a great deal of experimental data, the simulation results are in good agreement with the experimental data that shows the feasibility and predictability of the CA method.

Keywords Cellular automaton · Aluminum alloy · Microstructure evolution
Hot deformation

Introduction

Aluminum alloy with high strength and low density is applied widely in the field of aerospace industry [1]. The hot deformation is commonly used to process aluminum alloy. During hot deformation, aluminum alloy undergoes different cycles of heating, holding, deformation and cooling [2]. These physical processes significantly change the microstructure of the material and then affect the properties of the final products. In order to refine the microstructure and improve the mechanical properties, it is very important to control recrystallization volume fraction of the material [3].

Dynamic recrystallization behavior of aluminum alloy has been extensively studied. Han et al. [4] found that the increase of recrystallization fraction leads to lower strength and fracture toughness. Kannan and Raja [5] reported stress corrosion resistance of aluminum alloy can be improved by inhibiting recrystallization. Recrystallization has an adverse effect on the mechanical properties, occurrence of recrystallization can decrease strength, corrosion resistance and toughness [6].

The prediction and control of the microstructure is one of the most important problems in the modern aluminum industry [7]. With the fast development of computer and mathematical modeling, we can conduct microstructure modeling on mesoscale by different models such as CA method [8], Monte Carlo (MC) method [9] and Phase Field (PF) method [10] etc. CA method has become an important technique for predicting the evolution of microstructures. CA model can output the average grain size, the volume fraction of recrystallization and stress-strain curve etc. In addition, the morphology and distribution of the hot deformation microstructure can be obtained. CA method has been used to simulate dynamic recrystallization, static recrystallization and phase transformation successfully [11].

The hot deformation behavior of 7085 aluminum alloy was studied through the Gleeble experiments. A CA model is developed to simulate the dynamic recrystallization during hot compression. The CA model is validated by the experimental data, good agreement is found between the simulated and the experimental results.

Model Description and Experimental Details

Cellular automata are algorithms that simulate transformation of complex systems [12]. The transformation rules determine the state variable of a cell as a nonlinear function of the state variable of the cell itself and the state variable of the neighbouring sites. The automata of dynamic transformation occur though the application of transformation rules. For the purpose of simulating the DRX behavior of 7085 aluminum alloy, the simulation area is subdivided by an array of cells of 912×912 sites, they are made up of a regular lattice, the whole lattice corresponds to a real domain of $912 \mu\text{m} \times 912 \mu\text{m}$.

Model of Dislocation Density Evolution

There will be a lot of dislocation in the process of hot deformation. Generally, dislocations are produced by work hardening and disappeared by dynamic recrystallization. To simulate the deformation behavior and microstructure evolution of 7085 aluminum alloy, the Kocks-Mecking model has been used [13]:

$$\frac{d\rho_{i,j}}{ds} = K_1\sqrt{\rho_{i,j}} - K_2\rho_{i,j} \quad (1)$$

where K_1 is the parameter representing working hardening; K_2 is the parameter representing dynamic recovery and dynamic recrystallization, $\rho_{i,j}$ is the dislocation density of site (i, j) . It is assumed that the initial dislocation density is ρ_0 when $\varepsilon = 0$, with the boundary condition is presented (Eq. 9) can be expressed as:

$$\rho_{i,j} = \left(\frac{K_1}{K_2} - \frac{K_1}{K_z} e^{-\frac{K_2}{z}s} + \sqrt{\rho_0} e^{-\frac{K_z}{z}s} \right)^2 \quad (2)$$

The function of the flow stress and the mean dislocation density are as follows:

$$\bar{\rho} = \frac{1}{N_c} \sum_{i,j} \rho_{i,j} \quad (3)$$

$$\sigma = \alpha\mu b\sqrt{\bar{\rho}} \quad (4)$$

where N_c is the total number of the cells in the simulated space, b is the Burger's vector, $\bar{\rho}$ is the mean dislocation density, the correlation constant α is set to 0.5 in this article, μ is the shear modulus.

Model of Nucleation

As an important parameter of the thermal deformation process, the nucleation rate not only affects the recrystallized nucleation, but also has a great influence on the growth of recrystallized grain. The simulation of the nucleation process is based on a large number of experimental observation during the initial recrystallization process. The nucleation occurs mainly at grain boundaries. Many fine grain of equiaxed grains will appear at the grain boundary.

The critical dislocation density ρ_c is as follows [14]:

$$\rho_c = \left(\frac{80\gamma_k \dot{\epsilon}}{31M_k \mu^2 b^3} \right)^{1/3} \quad (5)$$

where γ_k is the grain boundary energy, μ is the shear modulus. The dislocation mean free path is calculated as:

$$l = \frac{k\mu b}{\sigma} \quad (6)$$

where k is a constant which is about 10 for most metals.

The microstructure evolution during hot compression deformation was simulated using probabilistic CA. The method has been widely used in the dynamic recrystallization of simulation. The normalized parameter P_{ij} at each site can be expressed as:

$$P_{ij} = \frac{1}{2} \frac{\rho_{ij} - \rho_{\min}}{\rho_{\max} - \rho_{\min}} \mu b^2 \quad (7)$$

where ρ_{ij} is the dislocation density at the site (i, j) , ρ_{\max} and ρ_{\min} are the maximum and minimum dislocation density, respectively.

In this article, we consider that the nucleation of fine equiaxed grain only occurs on old grain boundaries. For the cells that meet the criteria for nucleation, the state of the cell was changed, the whole system will be constantly updated. Many fine equiaxed grains appear at the grain boundary, the state variable of the cell was changed to be recrystallized. The rate of nucleation [15] can be expressed as:

$$\dot{N} = \frac{1}{4} C_0 \mu^2 b^2 (\rho_{ij} - \rho_c) \exp\left(-\frac{Q_{act}}{RT}\right) \quad (8)$$

where C_0 is a constant, Q_{act} is the activation energy for nucleation, R is the universal gas constant which is equal to 8.314, and T is the deformation temperature.

Model of Growth

After the emergence of the new equiaxed grains, the grain boundary moves outward, The new grain gradually grew up and the old grain gradually disappeared, the dislocation density gradually decreases in the process of nucleation and growth. The driving force of the recrystallized grain growth is derived from the storage energy produced by the deformation, the rate of recrystallized grain growth v can be calculated from the following equation:

$$v = mp \quad (9)$$

where m is the grain boundary mobility, and p is the driving force. We can get the grain boundary mobility by the following equation [16]:

$$m = m_0 \left(-\frac{Q_b}{kT} \right) \left\{ 1 - \exp \left[5 \left(\frac{\Delta\theta}{15} \right)^4 \right] \right\} \quad (10)$$

where Q_b is the activation energy, K is Boltzmanns constant, m_0 is a constant.

The driving force p can be calculated from the following equation:

$$p = \frac{1}{2} \mu b^2 \Delta\rho - \frac{2\gamma}{r} \quad (11)$$

where r is the average radius of the grain, τ is the line energy, $\Delta\rho$ is the difference of dislocation density, γ is the grain boundary energy. So it can be seen that driving force is related to a lot of factors.

The average radius of the grain can be expressed as [17]:

$$r = \sqrt{\frac{N_0 S}{\pi}} \quad (12)$$

where S is the area of a cell, N_0 is the number of cells, the number and area of the cell determine the average radius of the grain.

Experimental

The material for the experiments was aluminum ingot, the average grain size is about 100 μm . The chemical composition is similar to the composition of 7085 aluminum alloy shown in Table 1. The aluminum ingot was homogenized at 741 K for 36 h and then cool in water. To reduce the friction coefficient between the specimen and the press indenters, graphite was used as a lubricant in the isothermal compression test. The scheme of Gleeble tests is shown in Fig. 1, it is divided into

Table 1 Chemical composition of 7085 aluminum alloy

Elements	Zn	Mg	Cu	Zr	Cr	Fe	Mn	Si	Ti	Al
wt%	7.94	1.48	1.66	0.14	<0.01	<0.01	0.012	0.0028	<0.01	Bal.

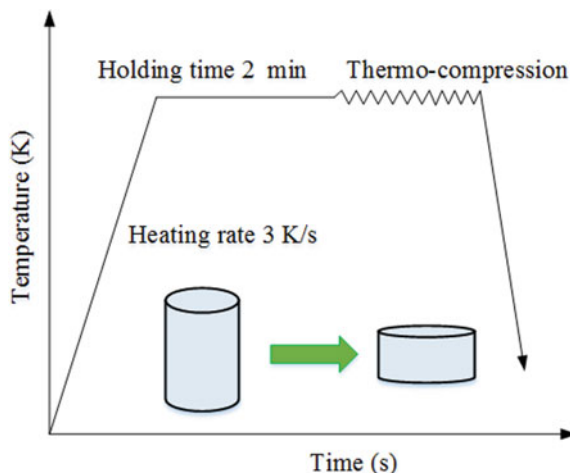


Fig. 1 The temperature-time curve of Gleeble test

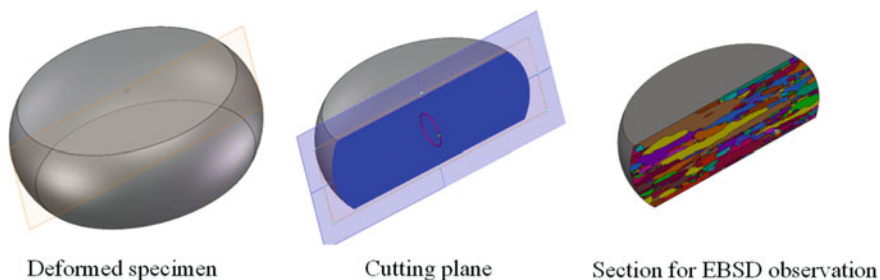


Fig. 2 Schematic representation for cutting plane of compressed samples

four stages: heating, heat preservation, compression and cooling, the heating rate is 3 K/s, holding time is 2 min, the specimens were quenched in water after deformation to freeze the as-deformed microstructure. As shown in Fig. 2, the deformed simple were sectioned for microstructure examination. Electron back scattered diffraction (EBSD) technique and optical microscopy (OM) were used to examine the specimens so as to obtain information about DRX.

Results and Discussion

The stress-strain curve of 7085 aluminum alloy obtained by hot compressive tests is shown in Fig. 3. The true stress-strain curve for DRX behavior can be divided into three stages: working-hardening stage, dynamic softening stage and steady state stage. The flow stress increases significantly to peak value caused by work hardening, and decreases attributed to the occurrence of dynamic recrystallization subsequently. The stress presents a steady state stage with the further increasing strain, the stress does not change violently with the change of strain. Which indicates the synergetic role of working hardening and dynamic softening.

The parameters used in this article are shown in Table 2.

Microstructural simulation of 7085 aluminum alloy was implemented using a large number Gleeble experimental parameters. To test the reasonableness of the model, The simulation results and the EBSD experimental results are compared and analyzed. Figure 4 shows the simulated microstructures and the experimental results. The different colors displays the different grain, the size and morphology of the grain between simulated microstructures and the experimental results are very similar.

Fig. 3 Three stage of true stress-strain curve

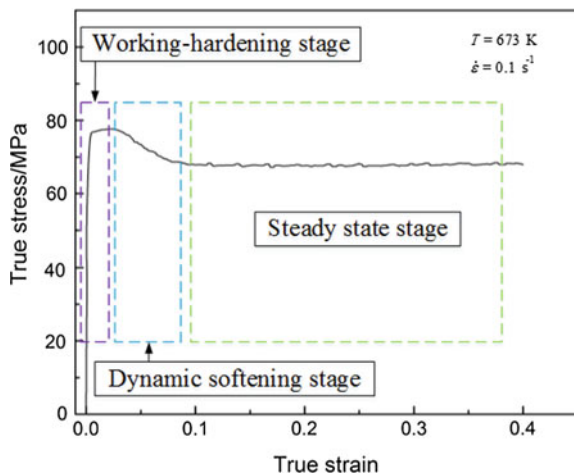


Table 2 Material constants for 7085 aluminum alloy

Parameters	Values
Q_{act} (kJ/mol)	313.386
Q_b (kJ/mol)	117.2
b (m)	2.0×10^{-10}
μ (MN/m ²)	2.69×10^4
D_{ob} (m ³ /s)	3.8×10^{-4}
T_m (K)	933.15
γ_m (J/m ²)	0.76

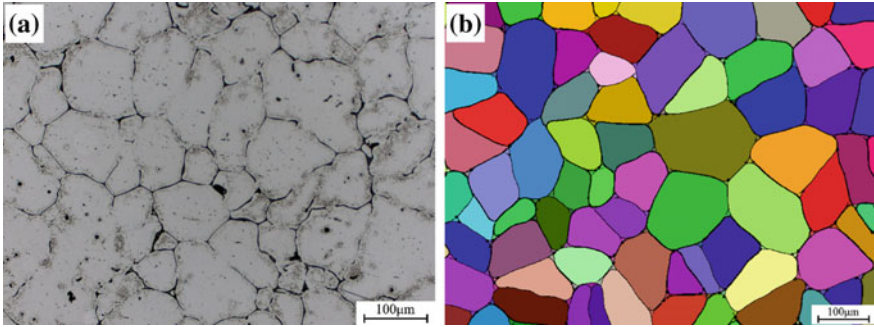


Fig. 4 Comparison of the initial microstructures obtained by **a** experimentation and **b** simulation

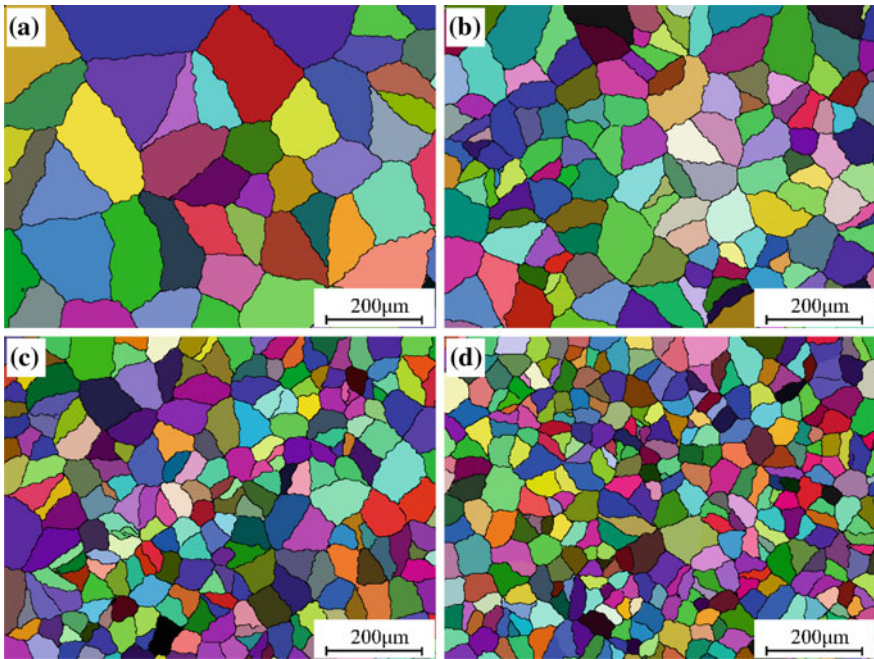


Fig. 5 Initial microstructure with different mean grain radii of **a** 200 μm . **b** 100 μm . **c** 50 μm . **d** 25 μm

In this article, the initial microstructures of different mean grain size were generated, all of them are equiaxed grains. Because the plastic deformation has not occurred yet, the density of dislocation is very low. It is found that the average grain radius is basically in accordance with the normal distribution by statistical data (Fig. 5).

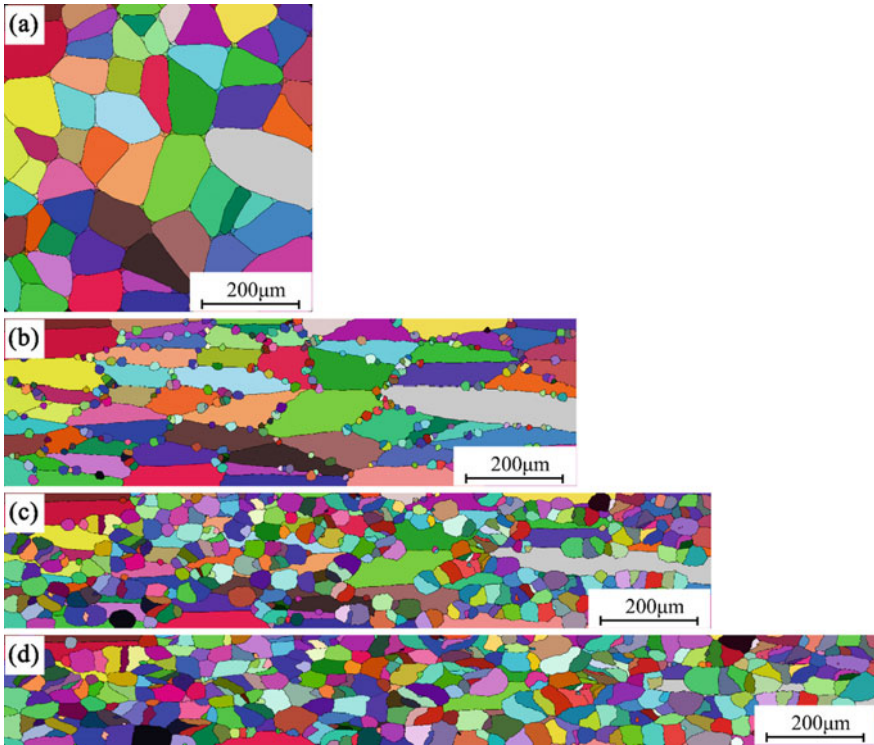


Fig. 6 The simulation results strain rate is 0.001 s^{-1} , temperature is 733 K. **a** $\varepsilon =$ initial microstructure. **b** $\varepsilon = 0.91$. **c** $\varepsilon = 1.20$ and **d** $\varepsilon = 1.38$

Figure 6 show the simulation results of 7085 aluminum alloy. The grain boundaries become slender, a large amount of deformation occurs in the grain. The nucleation of recrystallization mostly appearances at high angle grain boundaries, a lot of fine grain of equiaxed grains can be seen. The reason is that the energy is high at the grain boundary, recrystallization is easy to occur.

Figure 7 shows the process of the dynamic recrystallization with the deformation increase: the original grain suffer from plastic deformation and is elongated. During this period, the rapid increase of dislocation density, especially the disharmony between two adjacent grains, there will be a lot of dislocation at the grain boundary, subgrain boundaries is made up of dislocation, a large number of recrystallized grains will be produced at the old grain boundary. Eventually, these grains grow up slowly and the deformed coarse grain are replaced by fine equiaxed grains.

Figure 7 shows the microstructures of 7085 aluminum alloy. As the strain increases, the coarse grain is elongated. It can be observed that a great deal of recrystallized grains at the grain boundary. Moreover, there are some equiaxed grains appeared at triangle grain boundary, these grains grow up gradually in the follow-up process.

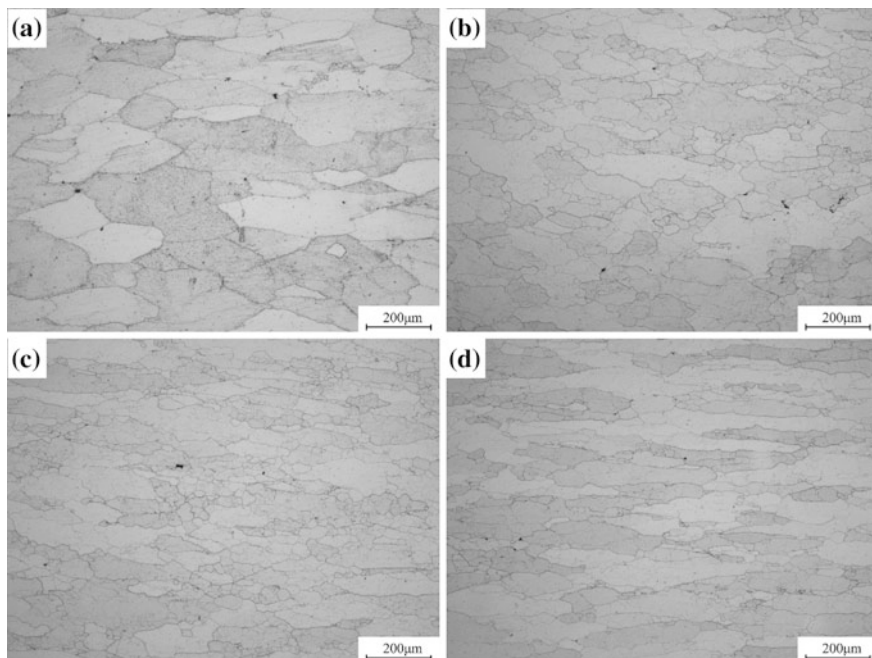


Fig. 7 Optical microstructures of 7085 aluminum alloy with **a** $\varepsilon = 0.51$. **b** $\varepsilon = 0.69$. **c** $\varepsilon = 0.91$. **d** $\varepsilon = 1.20$

Figure 8 shows the EBSD imaging maps of specimen deformed. A partially recrystallized necklace microstructure is observed in the Fig. 8. The small recrystallized grains delineated by high angle grain boundaries decorate on the old bulging grain boundaries, especially on triple junctions, indicating the initiation of DRX owing to the strain-induced boundaries migration. Meanwhile, some low angle grain boundaries that produced duo to dislocation generation and dislocation walls formation, are detected mainly at the vicinity of original grain boundaries.

From the diagram we can see the recrystallized microstructures from EBSD experiments, the deformed microstructures was not fully recrystallized in the 723 K and $\dot{\varepsilon} = 0.001 \text{ s}^{-1}$. By running the code at 723 K (Fig. 8) similar data are output indicating that CA model predicted recrystallized microstructure accurately. The strain rate, as an important parameter of the thermal deformation process, not only affects the recrystallized nucleation, but also has a great influence on the growth of recrystallized grain. The higher strain rate can obtain finer recrystallized grains at the grain boundary. The dynamic recrystallization fraction of the lower strain rate is higher, but the average grain radius of the grain is larger.

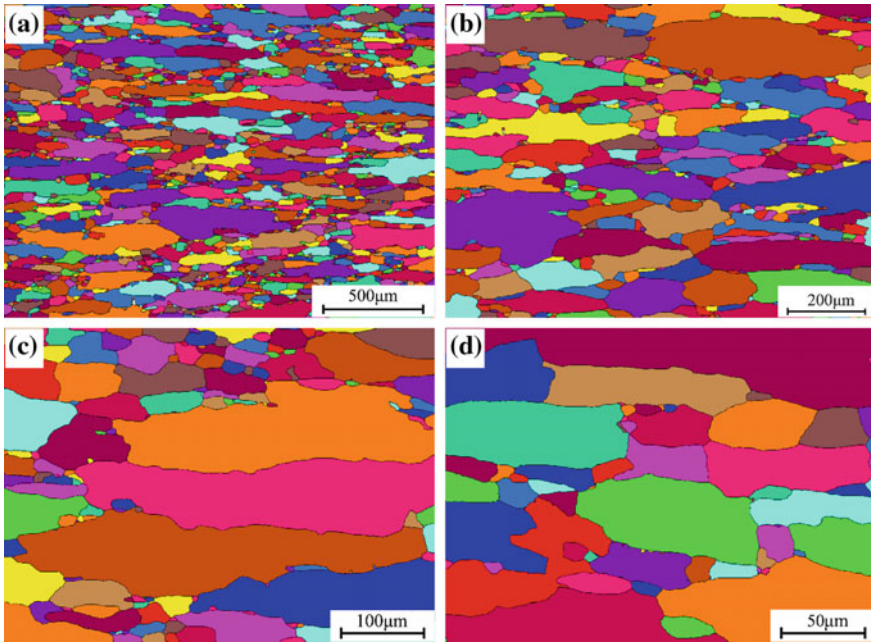


Fig. 8 EBSD imaging maps, strain is 1.20, temperature is 723 K and strain rate is 0.001 s^{-1} : **a** 50X. **b** 100X. **c** 200X. **d** 400X

Conclusions

The microstructure evolution of the 7085 aluminum alloy was researched by simulations and experiments. The simulation results can accurately reflect the actual process of dynamic recrystallization.

1. The fine equiaxed grains start to appear at the grain boundaries when suffering from plastic deformation, recrystallization happened easily where the dislocation density is very high. The dislocation density plays prominent part in DRX of 7085 aluminum alloy.
2. The strain have a major impact on the recrystallization volume percentage and the average grain size during DRX. When the deformation temperature and the strain rate are determined, the recrystallization volume percentage increases while the mean grain radius decreases slowly with the deformation increase. The higher the temperature, the smaller the average grain size, because the higher the temperature, the higher the activity of dislocation, which can provide more energy for recrystallization nucleation and growth.

3. The microstructure evolution of the 7085 aluminum alloy was simulated in different condition by a modified CA model. The CA simulated microstructure morphology was in good agreement with the results of EBSD observation. The relative error between the simulation results and the hot compression experimental results is very low. The CA method we developed can be used to simulate the microstructure changes during the thermal deformation process.

Acknowledgements This work was supported by the National Key and Development Program of China (No. 2016YFB0300803, 2016YFB0300903).

References

1. W. Liu, H. Zhao, D. Li, Z. Zhang, G. Huang, Q. Liu, Hot deformation behavior of AA7085 aluminum alloy during isothermal compression at elevated temperature, *Mater. Sci. Eng., A*, 596 (2015) 176–182.
2. C.Y. Lin, X.M. Chen, M.S. Chen, Y. Zhou, D.X. Wen, D.G. He, A new method to predict the metadynamic recrystallization behavior in a typical nickel-based superalloy, *Appl. Phys. A*, 122 (2016) 1–44.
3. M. Zouari, N. Bozzolo, R.E. Loge. Mean field modelling of dynamic and post-dynamic recrystallization during hot deformation of Inconel 718 in the absence of δ phase particles, *Mater. Sci. Eng. A*, 655 (2016) 408–424.
4. N.M. Han, X.M. Zhang, S.D. Liu, D.G. He, R. Zhang, Effect of solution treatment on the strength and fracture toughness of aluminum alloy 7050, *J. Alloys Compd.* 509 (2011) 4138–4145.
5. M.B. Kannan, V.S. Raja, Enhancing stress corrosion cracking resistance in Al-Zn-Mg-Cu-Zr alloy through inhibiting recrystallization, *Eng Fract Mech.* 77 (2010) 249–256.
6. D. Li, D.Z. Zhang, S.D. Liu, Z.J. Shan, X.M. Zhang, Q. Wang, Dynamic recrystallization behavior of 7085 aluminum alloy during hot deformation, *T Nonferr Metal Soc.* 26 (2016) 1491–1497.
7. D.S. Svyetlichnyy. Reorganization of cellular space during the modeling of the microstructure evolution by frontal cellular automata, *Comp Mater Sci.* 60 (2012) 153–162.
8. S.I. Kim, Y. Lee, D.L. Lee, Y.C. Yoo, Modeling of AGS and recrystallized fraction of microalloyed medium carbon steel during hot deformation, *Mater. Sci. Eng., A*, 355 (2003) 384–393.
9. B. Radhakrishnan, G. Sarma, T. Zacharia, Monte Carlo simulation of deformation substructure evolution during recrystallization, *Scripta Mater.* 39 (1998) 1639–1645.
10. T. Takaki, Y. Hisakuni, T. Hirouchi, A. Yamanaka, Y. Tomita, Multi-phase-field simulations for dynamic recrystallization, *Comp Mater Sci.* 45 (2009) 881–888.
11. C. Zheng, N. Xiao, D. Li, Y. Li, Microstructure prediction of the austenite recrystallization during multi-pass steel strip hot rolling: A cellular automaton modeling, *Comp Mater Sci.* 44 (2009) 507–514.
12. A. Timoshenkov, P. Warczok, M. Albu, J. Klarner, E. Kozeschnik, R. Bureau, Modelling the dynamic recrystallization in C-Mn micro-alloyed steel during thermo-mechanical treatment using cellular automata, *Comp Mater Sci.* 94 (2014) 85–94.
13. F. Chen, Z. Cui, J. Liu, W. Chen, S. Chen, Mesoscale simulation of the high-temperature austenitizing and dynamic recrystallization by coupling a cellular automaton with a topology deformation technique, *Mater. Sci. Eng., A*, 527 (2010) 5539–5549.
14. N. Shen, A. Samanta, H. Ding, Microstructure Simulations for Orthogonal Cutting via a Cellular Automaton Model, *Procedia CIRP.* 58 (2017) 543–548.

15. R. Ding, Z.X. Guo, Coupled quantitative simulation of microstructural evolution and plastic flow during dynamic recrystallization, *Acta Mater.* 49 (2001) 3163–3175.
16. F.J. Humphreys, A unified theory of recovery, recrystallization and grain growth, based on the stability and growth of cellular microstructures-I. The basic model, *Acta Mater.* 45 (1997) 4231–4240.
17. H. Hallberg, M. Wallin, M. Ristinmaa, Simulation of discontinuous dynamic recrystallization in pure Cu using a probabilistic cellular automaton, *Comp Mater Sci.* 49 (2010) 25–34.